

Sedimentary Organic Facies Division and Hydrocarbon-Generation Potential of Source Rocks in Coal-Bearing Strata—A Case Study of the Upper Paleozoic in Huanghua Depression, Bohai Basin, China

Chuanming Li, Jianhui Zeng,* Haitao Liu, Hongjun Li, Xiaoqing Bu, and Shuning Liu



Cite This: *ACS Omega* 2023, 8, 28715–28732



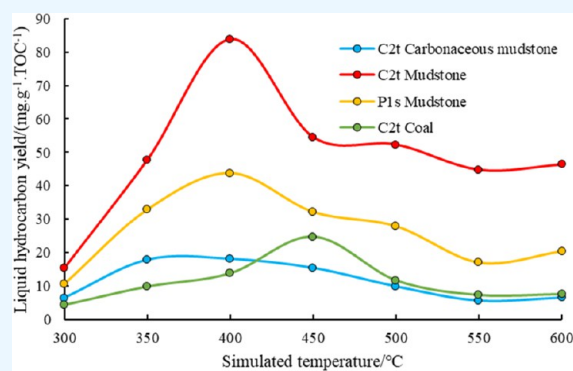
Read Online

ACCESS |

Metrics & More

Article Recommendations

ABSTRACT: Sedimentary organic facies cover the formation, evolution, and spatial distribution characteristics of organic matter, and they are effective tools for oil and gas resource evaluation and basin prospect prediction. According to the basic organic rock composition of the sedimentary organic facies, combined with the sedimentary facies and organic matter geochemical characteristics of Carboniferous–Permian strata, the characteristics of organic facies and hydrocarbon-generation potential of Upper Paleozoic source rocks in Huanghua Depression are being discussed. The results show that source rocks of Taiyuan and Shanxi Formations in the study area were oil-prone, and the oil-generation potential of mudstone is greater than that of carbonaceous mudstone and coal. The organic facies in the study area can be divided into six types: (1) terrestrial forest organic facies; (2) shallow swamp forest organic facies; (3) deep swamp forest organic facies; (4) deep swamp reed organic facies; (5) flowing water swamp organic facies; and (6) open water organic facies. The Taiyuan Formation is mainly composed of flowing water swamp, deep swamp forest, and shallow swamp forest with a strong hydrocarbon-generation capacity, while the Shanxi Formation chiefly includes organic facies of the deep swamp forest and shallow swamp forest. The deep swamp reed sedimentary organic facies had the highest hydrocarbon-generation potential, while the terrestrial forest sedimentary organic facies had the worst hydrocarbon-generation potential. Coal had a certain oil-generating capacity but was weaker than that of mudstone. Compared with mudstone, coal had a stronger gas-generating capacity.



1. INTRODUCTION

The concept of organic facies was given by Rogers in 1979 for the first time.¹ Since then, more and more attention has been paid to the study of organic facies, and the concept of organic facies has been expanded to sedimentary organic facies, which has rapidly become a new field of petroleum organic geochemistry.^{2–5} However, different scholars may have different understandings of the concept of organic facies, and their indicators for dividing organic facies may differ greatly.^{6–9} The origin and development of organic facies are closely related to coal petrology.^{6,10,11} Therefore, many scholars reveal the characteristics of source rock organic facies from the perspective of coal facies.^{12,13} Organic facies are classified according to the types of coal-forming marshes, and the indicators for the classification of organic facies focus on the characteristics of coal petrology.^{14,15} Based on the study of source rocks in the Turpan-Hami Basin and Junggar Basin, Jin divided the organic facies into dry swamp facies, forest swamp facies, flowing water swamp facies, and open water facies and applied them to the resource evaluation of coal-derived hydrocarbon, especially coal-derived oil.¹⁶ Oil and gas geochemists pay more attention to the hydrocarbon-generation

potential of source rocks, and the division of organic facies mainly reflects the degree of hydrogen richness and biological source characteristics of organic matter in geological bodies. For example, Jones divides organic facies into four main organic facies (A, B, C, D) and three transitional organic facies (AB, BC, CD) according to the hydrocarbon-generation potential, geochemical characteristics, and kerogen type of organic matter.¹⁷ Currently, the study of organic facies has started to focus on the sedimentary background of organic matter. Many scholars have divided the sedimentary organic facies of source rocks based on the sedimentary environment, sequence stratigraphy, organic matter type, biomarkers, and palynofacies, laying a foundation for the evaluation of oil and gas resources.

Received: May 16, 2023

Accepted: July 14, 2023

Published: July 24, 2023



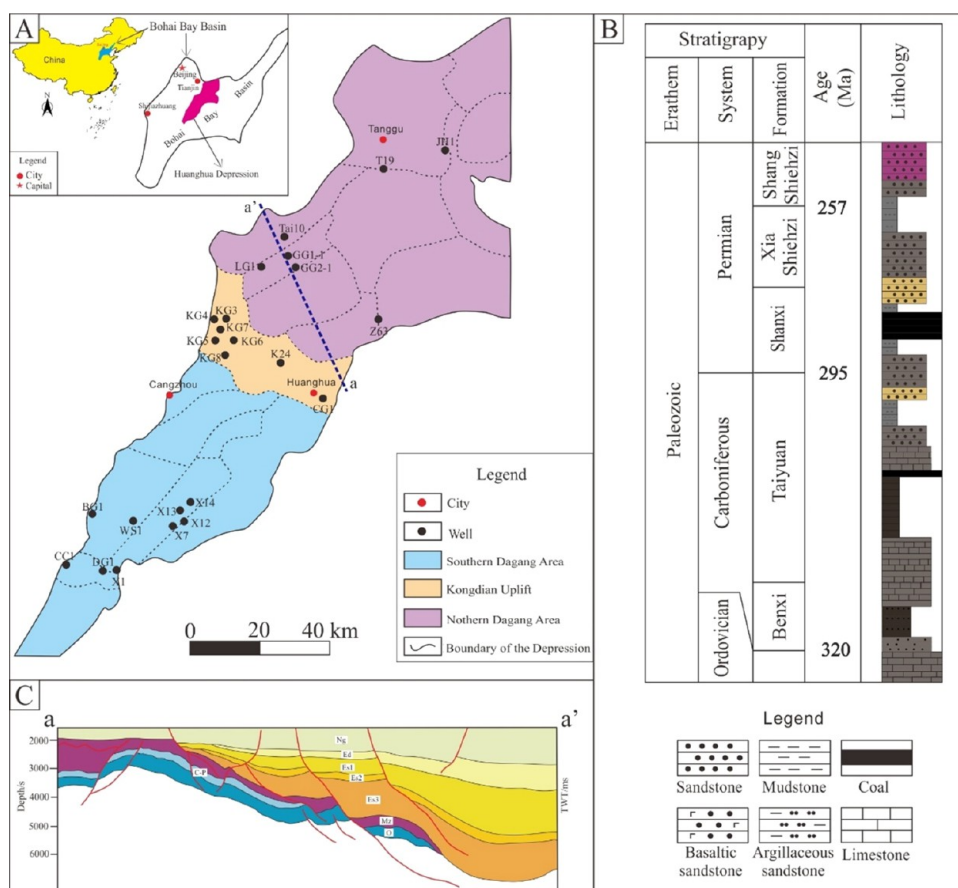


Figure 1. (A) Location map of the Huanghua Depression and (B) stratigraphic histogram. (C) a–a': geological profile in the Huanghua Depression.

The basic theory of sedimentary facies research comes from sedimentary petrology. Similarly, organic petrology is a significant theoretical basis and technical means for studying organic facies.^{6,10,12–14} The research contents of sedimentary organic facies include many factors such as the petrological characteristics, geochemical characteristics, biological characteristics, sedimentary environment of organic matter in sedimentary rock, and the distribution characteristics of sedimentary rock mass, among which the biological source characteristics of organic matter are the most important.^{5–11} It reflects not only the hydrocarbon-generation quality of organic matter but also its formation environment.^{15–17} The maceral, the most basic unit of organic petrology, is the basis for classifying organic matter types.^{12,13} The number of macerals directly reflects the abundance of organic matter in source rocks. The type and nature of macerals are the most direct indicators of the degree of evolution, hydrocarbon-generation potential, biological origin characteristics, and sedimentary environment of source rocks.¹⁸ The quantity of macerals directly reflects the abundance of organic matter in the source rocks. The optical properties and types of macerals are the most intuitive indicators of the degree of evolution, hydrocarbon-generation potential, biological source characteristics, and sedimentary environment of the source rocks.^{7–10} Consequently, the sedimentary organic facies classified on the basis of organic petrology can better reflect the quantity, type, maturity, and sedimentary environment of organic matter in geological bodies and their relationship with the types of hydrocarbon products that are genetically related to them.^{13–17}

The Carboniferous–Permian period of the Paleozoic is one of the important transition periods in the geological evolution history of the Bohai Bay Basin. During this period, a series of geologic historical events occurred, including rapid rise and fall of sea level, drastic change of climate, and abnormal carbon and sulfur isotopes.^{19,20} In the Middle–Late Carboniferous, due to the influence of the Hercynian movement and the crust subsidence, seawater intruded into the Bohai Bay basin on a large scale. In the Early Permian, transgression occurred only locally.²¹ In the Middle–Late Permian, seawater completely withdrew from the Bohai Bay Basin. In the transgressive and regressive environment, the sedimentary thickness of the Bohai Bay Basin is stable, and a set of continental–oceanic interaction and continental clastic deposits are developed.^{20–22} The complex sedimentary environment changes of the Carboniferous–Permian in the Bohai Bay Basin provided abundant and various biological sources for organic matter. In this paper, a comprehensive study of the organic facies of Carboniferous–Permian source rocks in the Huanghua Depression of the Bohai Bay Basin was conducted employing organic petrology, sedimentary facies, and organic geochemistry.

2. GEOLOGICAL SETTING

Located in the east of China, the Bohai Bay Basin is a petroleum basin with the largest oil and gas reserves and production in China, with an annual oil output of over 70 million tons.²¹ The Huanghua Depression is located at the "N"-type tectonic transition site in the middle of the Bohai Bay

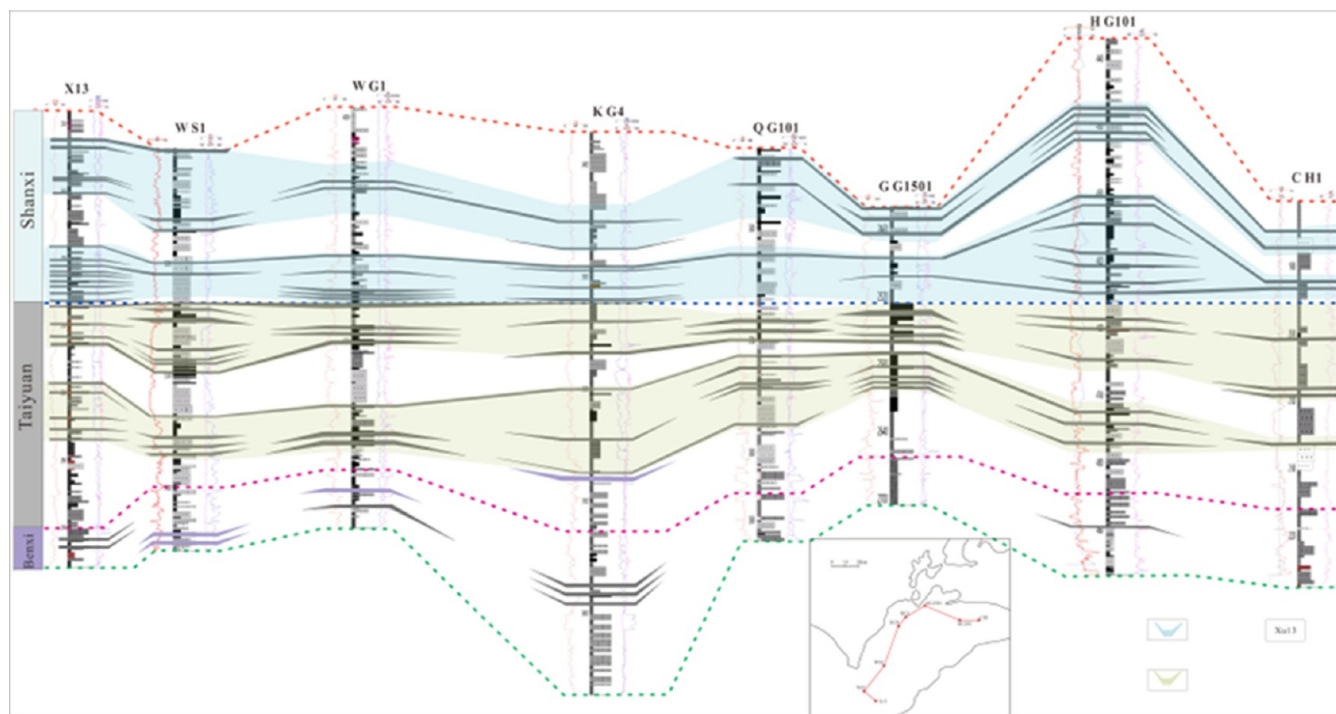


Figure 2. Spatial distribution characteristics of Upper Paleozoic coal measure source rocks in Huanghua Depression (modified after ref 25).

basin. It is distributed in the NNE direction. Its geographical location is $37^{\circ}37'–39^{\circ}50'$ north latitude and $116^{\circ}10'–119^{\circ}30'$ east longitude (Figure 1A).^{21,22} The Huanghua depression is divided into the Qikou depression, the Kongdian uplift, and the Cangdong depression from north to south. Qikou Sag and Cangdong Sag, as two main sags in the north and south, are composed of eight secondary sags and bulges (Figure 1A).^{22–24}

The Upper Paleozoic strata in Huanghua Depression are divided into the Benxi Formation (C_2b), Taiyuan Formation (C_2t), Shanxi Formation (P_1s), Xiashihezi Formation (P_{1x}), Shangshihezi Formation (P_2s), and Shiqianfeng Formation (P_{3s}) (Figure 1B). In the Late Paleozoic Taiyuan and Shanxi formations, four coal-accumulating phases were developed (Figure 2), forming widely developed coal measure source rocks,^{25,26} including three types: coal, carbonaceous mudstone, and mudstone.^{25,27,28} The source rock is generally thick in the south and thin in the north. The thickness of coal seams in the Taiyuan Formation ranges from 2 to 16 m, which is developed in a shallow marine sedimentary system. However, the coal seam thickness of the Shanxi Formation is 4–10 m, and it was developed in a delta sedimentary system. The cumulative thickness of dark mudstone is 230–420 m, and the total area is about 9600 km^2 .^{2,28,29}

Since Proterozoic, Huanghua Depression has experienced four stages of evolution: the Paleozoic platform stage, the Indosinian period of the north–south extrusion stage, the Yanshanian intraplate orogenic stage, and the complex rifting stages during Paleogene and Neogene.³⁰ Frequent tectonic movements have led to the development of faults in the study area, including deep and large faults connecting Paleozoic and Paleogene faults, and small faults in Paleozoic faults (Figure 1C).^{31,32} There have been lots of studies that have shown that oil and gas generated from the source rocks of the Upper Paleozoic migrated along faults to adjacent sandstone and carbonate reservoirs.^{30–32} In addition, the hydrocarbons in

Shahejie Formation of the upper Paleogene can also migrate into the upper Paleozoic reservoirs through faults, forming numerous types of inner buried-hill reservoirs.^{30–32}

3. DATE AND METHODS

3.1. Petrographic Analyses and Vitrinite Reflectance Determination. A total of 130 source rock samples (46 coal samples, 34 carbonaceous mudstone samples, and 50 dark mudstone samples) were collected from 26 boreholes. The DM LPWITH MSP200 reflective microscope was used to observe the petrological characteristics and measure the vitrinite reflectance. Executive standard: Petroleum and Natural Gas Industry Standard of the People's Republic of China (SY/T5124-1995)—Determination of Vitrinite Reflectance in Sedimentary Rock.³³ The quantification of maceral adopts the contrast method of reflection and fluorescence, which is realized under the PVGEOP program supported by Windows. Fluorescence analysis is performed using a 100 W ultra-high-pressure mercury lamp, BG3 + BG38 (violet light) excitation system, and a 490 nm blocking filter. The experiment follows relevant regulations of the International Commission on Coal and Organic Petrology (ICCP system, 1994).³⁴

3.2. Core Observation, Logging, and Well Logs. The logging curves in the study area mainly include acoustic time difference, resistivity, spontaneous potential, γ ray, density, and compensating neutron. Based on the sedimentary background of the Upper Paleozoic in the Bohai Bay Basin, the depositional environment of Upper Paleozoic source rocks in the study area can be judged by observing the lithology, color, structure, construction lithologic combination of the cores of key wells, combined with the characteristics and morphology of the logging curves of the corresponding wells.

3.3. Rock-Eval Pyrolysis and Total Organic Carbon (TOC). The pyrolysis test was carried out at an ambient temperature ($26 \text{ }^{\circ}\text{C}$) using an OGE-II rock pyrolysis

Table 1. Maceral Composition and Vitrinite Reflectance of Source Rocks from Different Areas in the Huanghua Depression, Bohai Bay Basin (on Mineral-Free Basis)^a

sample	formation	depth (m)	lithology	Ro (%)	Vit (%)	Int (%)	Exi (%)	Sap (%)
X13-1	C ₂ t	2769	coal		88.41	7.27	1.82	2.5
X13-2	C ₂ t	2771	coal		89.28	3.89	2.96	3.88
X13-3	C ₂ t	2900	coal		65.19	24.2	3.41	7.2
X13-4	C ₂ t	2760	coal		69.3	21.29	3.35	6.06
T10-1	C ₂ t	2820	coal		77.02	8.88	3.14	10.97
JH1-1	C ₂ t	2472	coal		89.46	5	1.57	3.97
GG2-1-1	C ₂ t	2895	coal		55.56	36.58	1.64	6.23
GG2-1-2	C ₂ t	3200	coal		71.14	9.91	8.6	10.35
KG4-1	C ₂ t	3559	coal	0.91	70.08	24.1	5.1	0
DG1-1	C ₂ t	2710	coal	1.38	70.5	29.5	0	0
WS1-1	C ₂ t	5250	coal	1.20	60.7	30.3	9	0
KG7-1	C ₂ t	3092	coal	0.88	73	10	14	3
X1-1	P ₁ s	3180	coal		79.64	8.64	5.2	6.52
X1-2	P ₁ s	3214	coal		42.34	39.96	8.05	9.65
DG1-2	P ₁ s	3394	coal	0.91	75.4	21.8	2.8	0
DG1-3	P ₁ s	3412	coal	0.90	75.4	24.6	0	0
WS1-2	P ₁ s	5370	coal	1.30	58.8	37	4.2	0
CS1-1	C ₂ t	1606	mudstone	1.52	64.2	35.6	0	0.2
CS1-2	C ₂ t	1620	mudstone	1.54	58.9	40.9	0	0.2
DG1-6	C ₂ t	3556	mudstone	1.19	75.8	24.2	0	0
DG1-7	C ₂ t	3553	mudstone	1.28	72.8	27	0	0.2
KG3-1	C ₂ t	3695	mudstone	0.81	62.3	28.4	8.5	0.8
KG3-2	C ₂ t	3720	mudstone	0.84	58.6	40.8	0.6	0
KG3-3	C ₂ t	3715	mudstone	0.90	61.5	34.9	2.4	1.2
KG8-1	C ₂ t	3430	mudstone	0.81				
KG8-2	C ₂ t	3456	mudstone	0.78				
X7-2	C ₂ t	1260	mudstone	0.80	70.2	14.6	8.8	6.4
X7-3	C ₂ t	1270	mudstone	0.79				
X7-4	C ₂ t	1286	mudstone	0.86	66.4	33.6	0	0
KG4-8	C ₂ t	3595	mudstone	0.79	75.4	11.4	8.6	4.6
KG4-9	C ₂ t	3598	mudstone	0.84	65.4	28.2	4.6	1.8
KG4-10	C ₂ t	3610	mudstone	0.80	65.4	19.3	10.1	5.2
KG4-11	C ₂ t	3622	mudstone	0.79	58	34.8	6.4	0.8
KG4-12	C ₂ t	3613	mudstone	0.79	72.3	19.3	2.2	6.2
KG4-13	C ₂ t	3619	mudstone	0.83	61.9	25.5	8.4	4.2
KG4-14	C ₂ t	3625	mudstone	0.86	58.8	34.2	5.8	1.2
KG4-15	C ₂ t	3630	mudstone	0.88	60.2	35.2	3.6	1
KG4-16	C ₂ t	3632	mudstone	0.90	70.2	19.2	3.4	7.2
KG4-17	C ₂ t	3636	mudstone	1.02	80.2	16	3.8	0
DG1-8	C ₂ t	3250	mudstone	1.08	81.2	18.6	0	0.2
DG1-9	C ₂ t	3225	mudstone	1.17	70.5	29.5	0	0
DG1-10	C ₂ t	3246	mudstone	1.21	80.1	13.5	6.4	0
DG1-11	C ₂ t	3236	mudstone	1.24	72.1	25.5	2.4	0
DG1-12	C ₂ t	3275	mudstone	1.40	65.4	34.6	0	0
WS1-4	C ₂ t	5243	mudstone	1.42	54.2	45.8	0	0
WS1-5	C ₂ t	5220	mudstone	1.38	62.4	37.2	0.4	0
WS1-6	C ₂ t	5226	mudstone	1.44	71.2	28.6	0	0
WS1-7	C ₂ t	5238	mudstone	1.39	38.4	61.6	0	0
X7-5	C ₂ t	3086	mudstone	0.84	42	47	8	3
X12-1	C ₂ t	1328	mudstone	0.85	67	25	8	0
KG6-2	C ₂ t	2488	mudstone	0.83	63	32	5	0
KG6-3	C ₂ t	2493	mudstone	0.85	79	15	6	0
X13-5	C ₂ t	2938	mudstone	0.91	73	15	12	0
X14-2	C ₂ t	2908	mudstone	0.79	84	5	10	1
KG7-1	C ₂ t	3589	mudstone	0.81	76	7	15	2
KG7-2	C ₂ t	3568	carbonaceous mudstone	0.85	74	12	14	0
KG5-3	C ₂ t	3428	mudstone	0.84	81	5	10	4
KG5-4	C ₂ t	3436	mudstone	0.81	59	34	7	0
KG5-5	C ₂ t	3430	carbonaceous mudstone	0.87	63	17	15	5
T19-1	C ₂ t	2980	mudstone	1.04	50	41	7	2

Table 1. continued

sample	formation	depth (m)	lithology	Ro (%)	Vit (%)	Int (%)	Exi (%)	Sap (%)
CS1-4	P _{1s}	1564	mudstone	1.24	66	28.5	4.7	0.8
CS1-5	P _{1s}	1549	mudstone	1.30	61.9	37.9	0.2	0
CS1-6	P _{1s}	1556	mudstone	1.40	71.2	28.2	0	0.6
DG1-13	P _{1s}	3145	mudstone	0.82	67.1	32.7	0	0.2
DG1-14	P _{1s}	3154	mudstone	0.93	58.6	41.4	0	0
KG5-6	P _{1s}	3326	mudstone	0.81	51.4	44	0.4	4.2
KG5-7	P _{1s}	3358	mudstone	0.78	82.4	17.6	0	0
KG4-18	P _{1s}	3546	mudstone	0.81	57.6	24.2	18.2	0
KG4-19	P _{1s}	3549	mudstone	0.83	60.5	37.1	2.4	0
KG4-20	P _{1s}	3556	mudstone	0.82	66.4	28.8	4.8	0
KG4-21	P _{1s}	3559	mudstone	0.78	63.7	21.4	8.1	6.8
KG4-22	P _{1s}	3570	mudstone	0.85	64.8	30.2	5	0
DG1-15	P _{1s}	3160	mudstone	0.85	60.5	34.5	5	0
DG1-16	P _{1s}	3162	mudstone	0.82	81.2	15.4	3.4	0
DG1-17	P _{1s}	3170	mudstone	0.84	61.4	37.1	1.1	0.4
WS1-8	P _{1s}	5102	mudstone	0.88	64.8	32.5	2.7	0
WS1-9	P _{1s}	5121	mudstone	0.96	58.4	36.5	5.1	0
WS1-10	P _{1s}	5126	mudstone	1.02	60.4	39.6	0	0
WS1-11	P _{1s}	5124	mudstone	0.92	54.8	41.3	3.9	0
WS1-12	P _{1s}	5130	mudstone	0.99	30.8	69.2	0	0
WS1-13	P _{1s}	5133	mudstone	1.02	42.4	57.6	0	0
WS1-14	P _{1s}	5134	mudstone	0.14	50.8	49.2	0	0
WS1-15	P _{1s}	5139	mudstone	1.08	54.6	45.4	0	0
WS1-16	P _{1s}	5147	mudstone	1.10	57.2	42.8	0	0
WS1-17	P _{1s}	5149	mudstone	1.06	70.5	21.8	7.7	0
WS1-18	P _{1s}	5150	mudstone	1.08	67.2	32	0.8	0
WS1-19	P _{1s}	5151	mudstone	1.10	48.2	51.8	0	0
WS1-20	P _{1s}	5153	mudstone	1.12	59.8	38.7	1.1	0.4
WS1-21	P _{1s}	5456	mudstone	1.18	62.8	27.7	8.7	0.8
WS1-22	P _{1s}	5159	mudstone	1.24	62.4	37.6	0	0
WS1-23	P _{1s}	5160	mudstone	1.28	70.2	29	0.8	0
Z63-1	P _{1s}	3456	mudstone	1.24	69	24	7	0
X14-3	P _{1s}	2842	mudstone	0.82	70	22	8	0
X14-4	P _{1s}	2851	mudstone	0.85	82	14	4	0
KG7-3	P _{1s}	2976	mudstone	0.81	59	35	6	0
KG6-4	P _{1s}	2354	carbonaceous mudstone	0.80	64	15	13	8

^aNote: C₂t, Taiyuan Formation; P_{1s}, Shanxi Formation; Vit, vitrinite; Int, inertinite; Exi, exinite; Sap, sapropelite; and Ro, vitrinite reflectance.

instrument. First, we heat the sample to 300 °C and perform thermal desorption analysis on the rock to measure the free soluble hydrocarbon peak (P₁). Then, we heat the sample to 500 °C, and the pyrolysis hydrocarbon peak (P₂) was obtained by thermal cracking analysis. Finally, the soluble hydrocarbon content S₁, the pyrolysis hydrocarbon content S₂, and the pyrolysis peak temperature T_{max} were calculated from the peak areas of P₁ and P₂. The TOC (total organic carbon) was measured by LECO CS230. After crushing, the sample was passed through a sieve with a pore size of less than 0.2 mm and was soaked in hydrochloric acid with a volume ratio of 1:7 for more than 2 h to eliminate the carbonates. After confirming that there was no residual carbonate component, the sample was put into a constant-temperature drying oven for use. The test is carried out in accordance with the national standard GB/T18062-2012 of the People's Republic of China.³⁵

3.4. Hydrous Pyrolysis. Fresh core samples of coal, mudstone, and carbonaceous mudstone from well GG1612 were utilized to conduct hydrocarbon-generation simulation experiments. The samples were pulverized below 200 mesh, the fines removed, and divided into six equal parts, 8 g each. Before the experiment, the experimental vessel was flushed

with helium gas to remove the air. The gold tube containing the sample was placed in an autoclave, and 15 mL of distilled water was injected into each part of the sample through a high-pressure pump. Then, each part of the coal was heated at a rate of 40 °C/h to 300, 350, 400, 450, and 500 °C, respectively. Mudstone and carbonaceous mudstone were heated to 350, 400, 450, 500, and 550 °C, respectively. The gas generated in the gold tube in the thermal simulation experiment was released, and the light hydrocarbon liquid products were separated by using a vacuum glass apparatus.

4. RESULTS AND DISCUSSION

4.1. Organic Petrological Characteristics. The macerals of the Upper Paleozoic coal, dark mudstone, and carbonaceous mudstone samples in the study area were analyzed. The organic maceral composition and vitrinite reflectance data of the samples are shown in Table 1.

4.1.1. Types of Organic Matter in Source Rocks. Research on the type of organic matter in the study area mainly uses the optical method to determine the type of kerogen, and at the same time, according to the pyrolysis data, the pyrolysis method is also utilized for the determination. Mutual

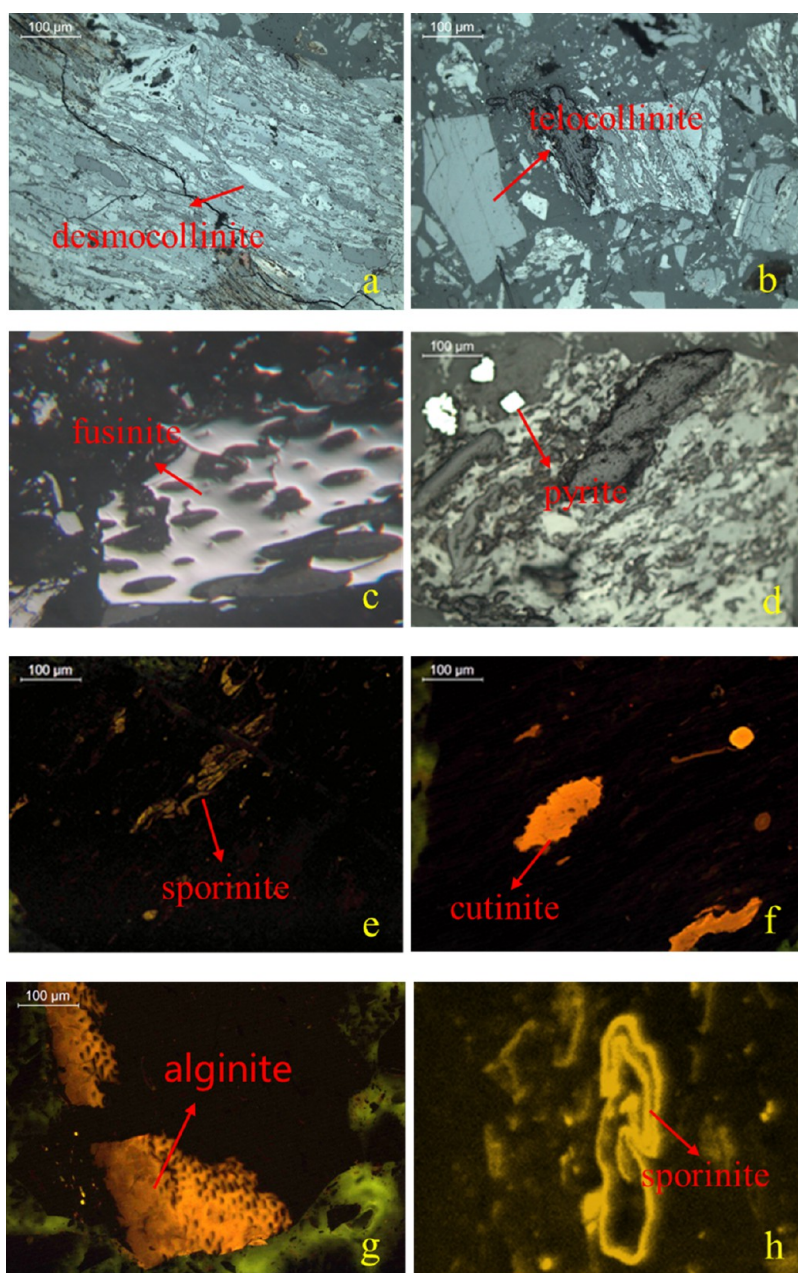


Figure 3. Photomicrographs of macerals observed in the study area. (a) Desmocollinite of coals in Carboniferous of the Taiyuan Formation, Chenghai 1, (b) telocollinite of coals in Carboniferous of the Taiyuan Formation, Chenghai 1, (c) fusinite of coals in Permian of the Shanxi Formation, Donggu 1, (d) pyrite of coals in Carboniferous of the Taiyuan Formation, Ganggu 2-1, (e) sporophyte, coal, Shanxi Formation, Permian, well Chenghai 24, (f) cutinite, coal, Taiyuan Formation, Carboniferous, well Banshen 1-1, (g) alginite, coal, Taiyuan Formation, Carboniferous, well Banshen 1-1, and (h) sporophyte, coal, Taiyuan Formation, Carboniferous, well Wanggu 1.

corroboration and complementation of two kinds of methods make it highly credible. According to the microscopic observation of the source rocks in the study area (Figure 3), the maceral of the source rocks is mainly vitrinite, which shows that they have undergone strong gelatinization before coal formation. Desmocollinite has various shapes (Figure 3a), and the bands of different widths are the most common, which are grayish white under the reflected light of oil immersion. Telocollinite is gray under oil-immersed reflected light (Figure 3b), principally in the form of lumps and strips, uniform and pure. In the exinite group, sporinite (Figure 3h) and cuticle (Figure 3f) are more common, and alginite (Figure 3g) and cork plastids can also be seen, which are mostly yellow and

orange under fluorescent illumination. Fusinite is the most common in the inertinite (Figure 3c,e), with clear cell walls and intercellular spaces, bright white under oil-immersed reflected light, basically showing the original structure of preburning plants (Figure 3d).

By analyzing the pyrolysis data of the source rock in the study area (Figure 4), it was found that the kerogen in the source rock of the study area is mainly of type II₁, type II₂, and type III. Type III kerogen only exists in the strata of the Shanxi Formation. At the same time, a large number of type II₂ kerogens also develop in the source rocks of the Shanxi Formation. The source rocks of the Taiyuan Formation are dominated by type II₁ and type II₂ kerogens, with a small

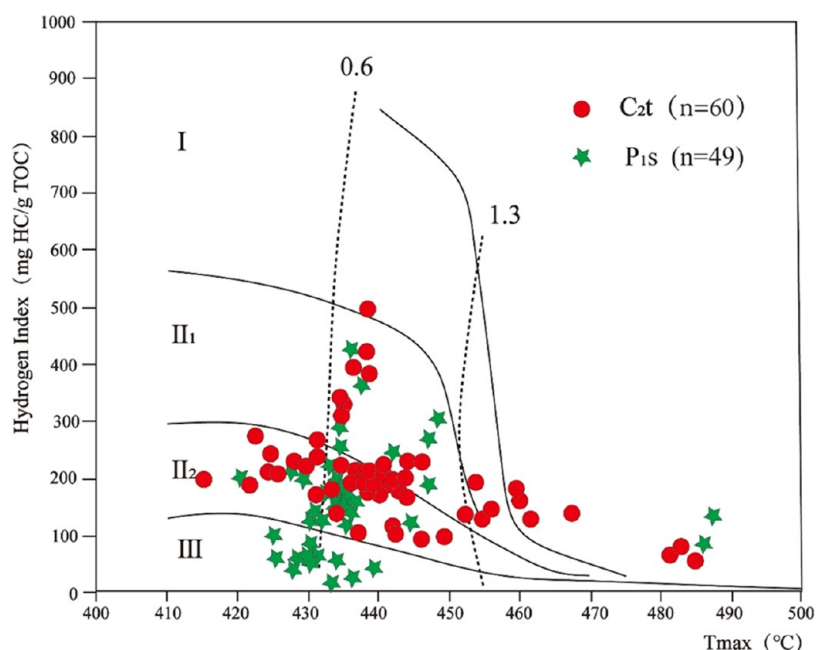


Figure 4. Type discrimination of Upper Paleozoic source rock in the study area (Base map according to ref 36).

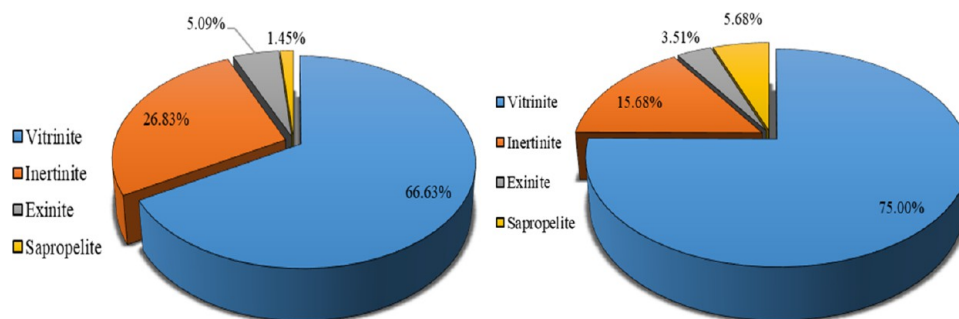


Figure 5. Maceral distribution of mudstone (left) and coal (right) in Taiyuan Formation of Huanghua Depression.

amount of type I kerogens. The results of the pyrolysis data analysis are basically consistent with those observed under a microscope.

4.1.2. Maceral Content Characteristics. 4.1.2.1.. *Maceral Content Characteristics of Source Rocks in Taiyuan Formation.* The maceral characteristics of coal, mudstone, and carbonaceous mud are illustrated in Figures 5 and 6. The vitrinite, exinite, and sapropelite in this formation have a high content, while the inertinite has a low content. Compared with

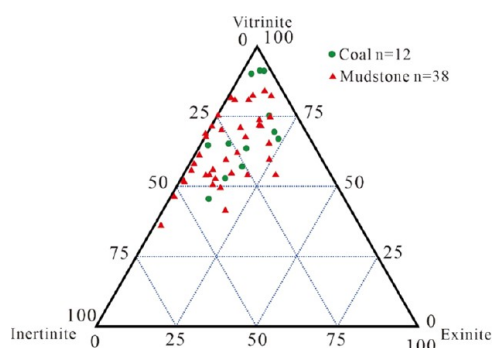


Figure 6. Triangular map of microcomponents of source rocks of Taiyuan Formation in Huanghua Depression.

mudstone, coal has a higher vitrinite content (75% on average) and sapropelite content (5.68% on average), but its exinite content is lower than mudstone.

4.1.2.2.. *Maceral Content Characteristics of Source Rocks in Shanxi Formation.* The contents of vitrinite, inertinite, and exinite are the highest in the source rocks of the Shanxi Formation. The sapropelite has the lowest content (Figures 7 and 8). The vitrinite and sapropelite of coal are obviously higher than those of mudstone, and the content of exinite of the two is similar. Compared with the coal of the Taiyuan Formation, the content of vitrinite and exinite of the Shanxi Formation is lower, and the content of sapropelite is basically the same as that of the Taiyuan Formation. The contents of vitrinite, exinite, and sapropelite in mudstone of the Taiyuan Formation are higher than those of the Shanxi Formation. On the whole, the hydrocarbon-generating capacity of the Taiyuan Formation source rocks is better than that of the Shanxi Formation.

4.2.. Geochemical Characteristics. 4.2.1.. *Organic Matter Content.* The organic matter in source rocks is the basic material for generating oil and gas. Therefore, the content and distribution characteristics of organic matter in source rocks are the basic indexes for evaluating source rocks. However, over a long period of geological history, there was no method to measure the original abundance of organic matter. Since

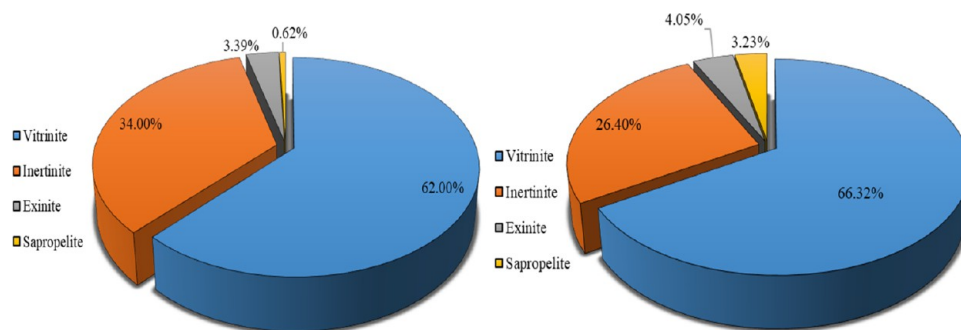


Figure 7. Maceral distribution of mudstone (left) and coal (right) of Shanxi Formation in Huanghua Depression.

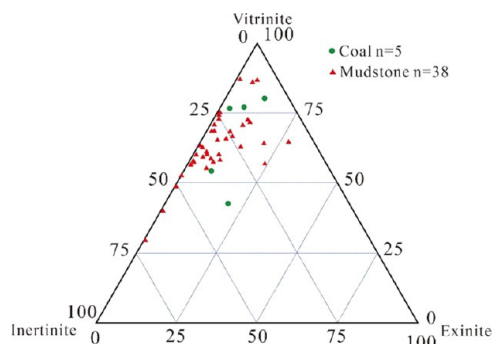


Figure 8. Triangular map of microcomponents of source rocks of Shanxi Formation in Huanghua Depression.

only a small quantity of organic matter in source rocks is converted into oil or natural gas, the original organic matter abundance can be indicated by the residual organic matter abundance.³⁷ Indicators such as total organic carbon content (TOC), chloroform asphalt "A" content, total hydrocarbon content (HC), and hydrocarbon-generation potential of organic matter pyrolysis ($S_1 + S_2$) are commonly used to evaluate the abundance of organic matter in source rocks.³⁷ The source rocks of the Upper Paleozoic in the Huanghua Depression are mainly developed in the strata of the Taiyuan and Shanxi Formations. Therefore, the source rocks of the Taiyuan Formation and Shanxi Formation are mainly studied in this study.

4.2.1.1.. Hydrocarbon-Generation Potential. The hydrocarbon-generation capacity of different lithologic source rocks in the study area is quite different (Table 2). The hydrocarbon-generation potential of coal is the largest (with an average of 82.13 mg/g), followed by that of carbonaceous mudstone (with an average of 22.41 mg/g), and that of mudstone is the smallest (with an average of 3.04 mg/g). The hydrocarbon-generation potential of the Taiyuan Formation source rock (mudstone, carbonaceous mudstone, and coal) is greater than that of the Shanxi Formation source rock in which the hydrocarbon-generation potential of Taiyuan Formation coal is

the largest (with an average of 92.91 mg/g) and that of Shanxi Formation mudstone is the smallest (with an average of 3.01 mg/g).

The mudstone, carbonaceous mudstone, and coal in the study area all show good hydrocarbon-generation ability (Figure 9),³⁶ The hydrocarbon-generation ability of the source rocks in the study area is evaluated according to the hydrocarbon-generation potential and hydrogen index chart. The results show that the source rocks of Upper Paleozoic in Huanghua Depression are generally of medium to very good quality in terms of hydrocarbon-generation capacity. The hydrocarbon-generation capacity of Taiyuan Formation source rocks is generally better than that of Shanxi Formation source rocks, and the hydrocarbon-generation capacity of coal is superior to that of mudstone and carbonaceous mudstone.

4.2.1.2.. Total Organic Carbon (TOC) Content. The TOC content of Upper Paleozoic mudstone in the study area ranges from 0.29 to 5.77%, with an average value of 2.56%. The TOC content of carbonaceous mudstone ranges from 6.05 to 24.36%, with an average value of 11.63%. The TOC content of coal ranges from 25.39 to 73.96%, with an average value of 44.73%. The average TOC contents of carbonaceous mudstone and coal in the Taiyuan Formation are 13.2 and 46.78%, respectively, which are higher than those in the Shanxi Formation. However, the average TOC content of mudstone in the Taiyuan Formation is only 2.35%, which is lower than that in the Shanxi Formation. Horizontally, the mean organic carbon content of the Kongnan, Beidagang, Wumaying, and Wangguantun areas is higher than that of other areas, and the average organic carbon content of mudstone is higher than 4% (Figure 10).

4.2.1.3.. Chloroform Asphalt "A". Chloroform asphalt "A" refers to the general term for the chloroform-soluble organic matter in the rock, which generally accounts for 2–15% of the organic matter. It is a mixture from which four components of saturated hydrocarbons, aromatic hydrocarbons, non-hydrocarbons (gums), and asphaltenes can be separated. Among them, the sum of the content of saturated hydrocarbons and aromatic hydrocarbons in the rock is called the total

Table 2. Organic Matter Abundance Statistics of Source Rocks in the Study Area^a

sample type	C ₂ t			P ₁ s		
	mudstone	carbonaceous mudstones	coal	mudstone	carbonaceous mudstones	coal
$S_1 + S_2$ (mg/g)	3.1 0.44 – 14.49	25.4 0.39 – 93.88	92.91 1.3 – 164.61	3.01 0.18 – 6.49	18.83 0.47 – 112.1	69.91 1.94 – 114.07
TOC (%)	2.35 0.44 – 5.17	13.2 6.52 – 24.36	46.78 25.39 – 73.96	2.84 0.29 – 5.77	9.76 6.05 – 20.3	42.41 27.2 – 70.57

^aNote: $\frac{\text{average value}}{\text{minimum value} - \text{maximum value}}$.

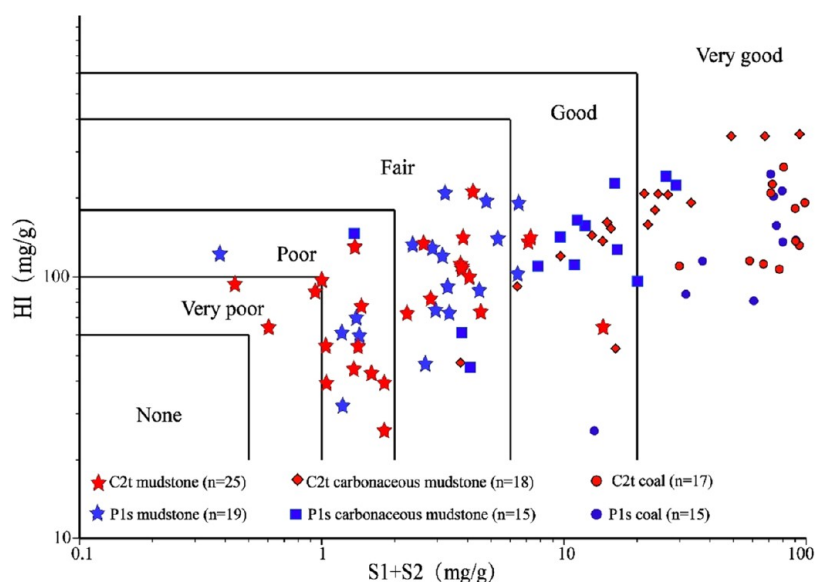


Figure 9. Evaluation chart of Upper Paleozoic source rocks in Huanghua Depression (Base map according to ref 36).

hydrocarbon content (HC). The content of chloroform asphalt "A" can reflect not only the abundance of organic matter but also the degree of conversion of organic matter to petroleum.^{34–36}

In this paper, the chloroform asphalt "A" of the source rocks in the Xiashihezi Formation, Shanxi, and Taiyuan Formations of the Ganggu 16102 well in the study area was tested and analyzed. The samples include three lithologies: coal, mudstone, and carbonaceous mudstone. The average value of the samples is 0.159%, the minimum value is 0.0014%, and the maximum value is 1.74%. The maximum value appears in the coal seam of the Taiyuan Formation, and the minimum value appears in the strata of the Xiashihezi Formation. The average content of chloroform asphalt "A" of mudstone in the Shanxi Formation is 0.008%, and there are no coal and carbonaceous mudstone sample data available. The average content of chloroform asphalt "A" is 0.012% in the Taiyuan Formation mudstone, 0.09% in the carbonaceous mudstone, and 1.18% in coal. Referring to the commonly used evaluation standard of source rock abundance, the average value of chloroform asphalt "A" of the source rocks in the Taiyuan Formation in the study area is 0.3%, which is generally a good source rock, while the average value of the source rocks in the Shanxi Formation is 0.25%, inferior to the source rocks of the Taiyuan Formation, which is also a good source rock.

4.2.2. Maturity of Organic Matter in Source Rocks. The maturity of organic matter refers to the degree of the thermal evolution of organic matter in source rocks. Since oil and natural gas are only formed in certain evolutionary stages of organic matter, maturity is also one of the important parameters for evaluating source rocks. The indicators used to determine maturity generally include three aspects: organic geochemistry, organic petrology, and direct measurement of paleotemperature.³⁴

In this paper, the source rock maturity is determined mainly by the vitrinite reflectance of the source rock. After sorting and analyzing the Ro data of its coal-bearing source rocks, it is believed that the Ro value of the Carboniferous and Permian coal-bearing strata in the study area is between 0.55 and 3.73% (Figure 11). Due to the influence of volcanic baking (Figure 12),^{36,38,39} the southern part of the study area has a high Ro

value of up to 2.5%, and the northern Zhangjuhe area is also relatively high, up to 3.73%, as shown in Figure 13. Vertically, the thermal evolution degree of coal-bearing source rocks within 3400 m does not change significantly, while there is a positive correlation after 3400 m.

4.3. Division of Sedimentary Organic Facies.

4.3.1. Classification of Organic Facies Types. Sedimentary organic facies are a symbiotic assemblage of organic matter formed under different sedimentary environments and evolutionary conditions. As a kind of organic component, they have not only specific petrology characteristics but also certain geochemical characteristics.^{2,40,41} Therefore, different sedimentary organic facies have dual properties of petrology and geochemistry and different hydrocarbon-generation characteristics. They are also the basis for using petrological and geochemical characteristics to reflect sedimentary organic facies and their distribution and to evaluate favorable exploration areas.^{10,11}

Throughout the research on coal facies and sedimentary organic facies at home and abroad, it has been studied from the perspective of coal science, paleobotany, geochemistry, and sedimentology. Coal facies are the manifestation of peat material deposited in a certain environment, which is the original genetic type of coal. They are indicated by maceral and mineral content as well as some structural features, and they reflect different hydrocarbon-generation types of source rocks. Although there are still many problems in the application of genetic parameters of coal maceral, the gelatification index (GI) and plant tissue preservation index (TPI) proposed by Diessel are still the most widely used indicators to characterize the microenvironment in the process of peat accumulation in coal facies analysis.¹³ Their expressions are as follows

$$GI = \frac{\text{vitrinite} + \text{macrinite}}{\text{fusinite} + \text{semifusinite} + \text{inertodetrinite}} \quad (1)$$

$$TPI = \frac{\text{telovitrinite} + \text{telocollinite} + \text{fusinite} + \text{semifusinite}}{\text{desmocollinite} + \text{macrinite} + \text{inertodetrinite}} \quad (2)$$

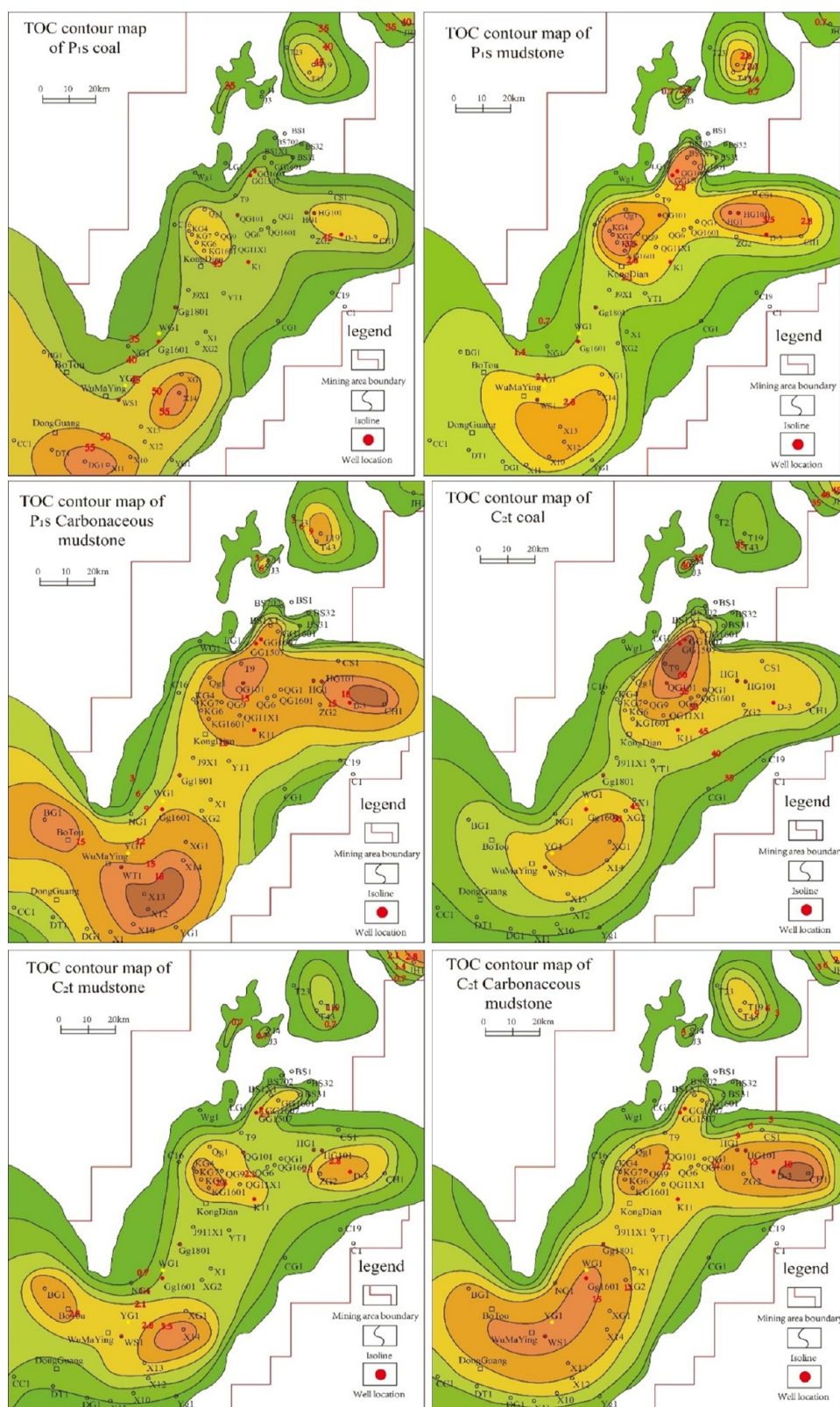


Figure 10. TOC contour map of Upper Paleozoic source rocks in Huanghua Depression.

The gelation index (GI) is the ratio of the gelatinous component to nongelled components, which mainly reflects the water level of ancient peat swamps. The plant tissue preservation index (TPI) is a reflection of microbial degradation, gelation, and natural fragmentation of plant

remains. In addition, the ratio of vitrinite to inertinite (V/I) parameter can reflect the degree of oxidation of the peat swamp that coal formed. The mobility index (MI) reflects the mobility of the water body during peat swamp accumulation. Its expression is as follows

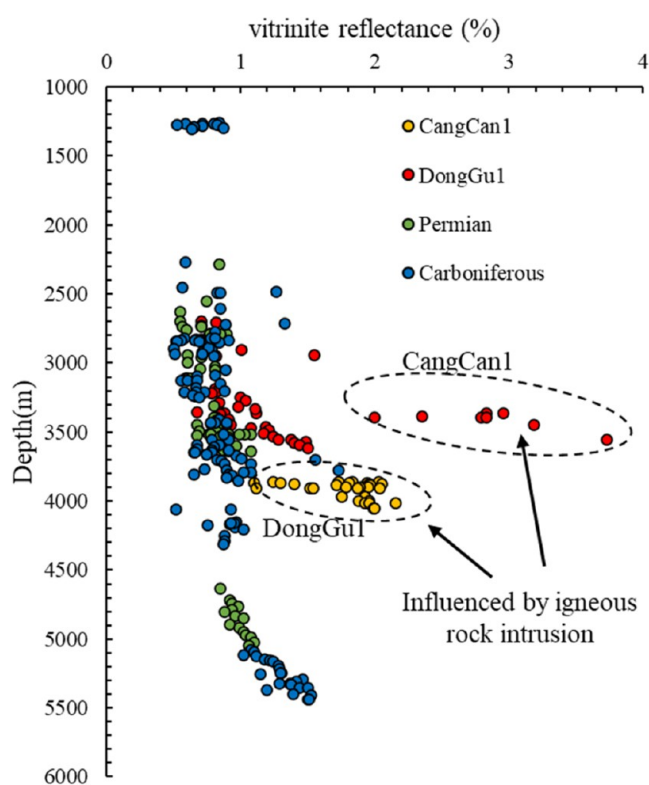


Figure 11. Relationship between R_o and well depth of the Carboniferous–Permian source rock in Huanghua Depression.

$$MI = \frac{\text{detrovitrinite} + \text{inertodetrinite} + \text{exinite}}{\text{desmocollinite} + \text{telocollinite}} \quad (3)$$

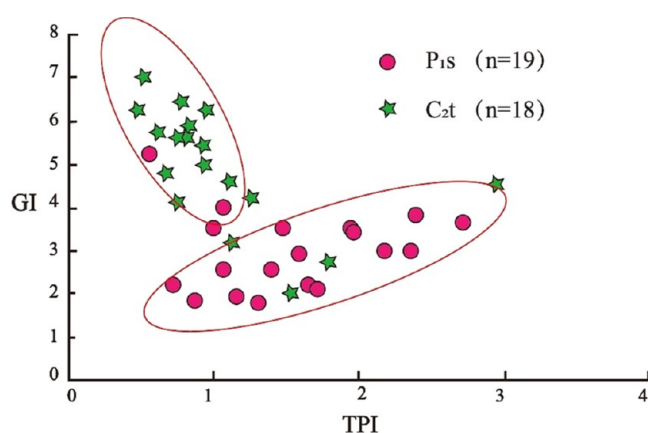


Figure 13. TPI-GI distribution characteristics of coal.

The Carboniferous–Permian coal measures in North China were formed in a vast epicontinental sea. Their sedimentary environment, hydrodynamic conditions of the medium, redox properties, and paleoplant (fossil plant) types are significantly different from those of Jurassic coal-bearing strata formed in large inland lacustrine basins such as the Turpan-Hami Basin and Junggar Basin.^{14,42,43} As shown in Figure 13, it can be seen that the coal of the Taiyuan Formation in the study area has a higher gelation index than that of the Shanxi Formation, but its tissue preservation index is lower than that of the coal of the Shanxi Formation.⁴⁴ This indicates that the coal of the Taiyuan Formation is formed in a swamp that is covered by deep water.

The division of the sedimentary organic facies of the Carboniferous–Permian coal-bearing source rocks in the Huanghua Depression is mainly based on the characteristics

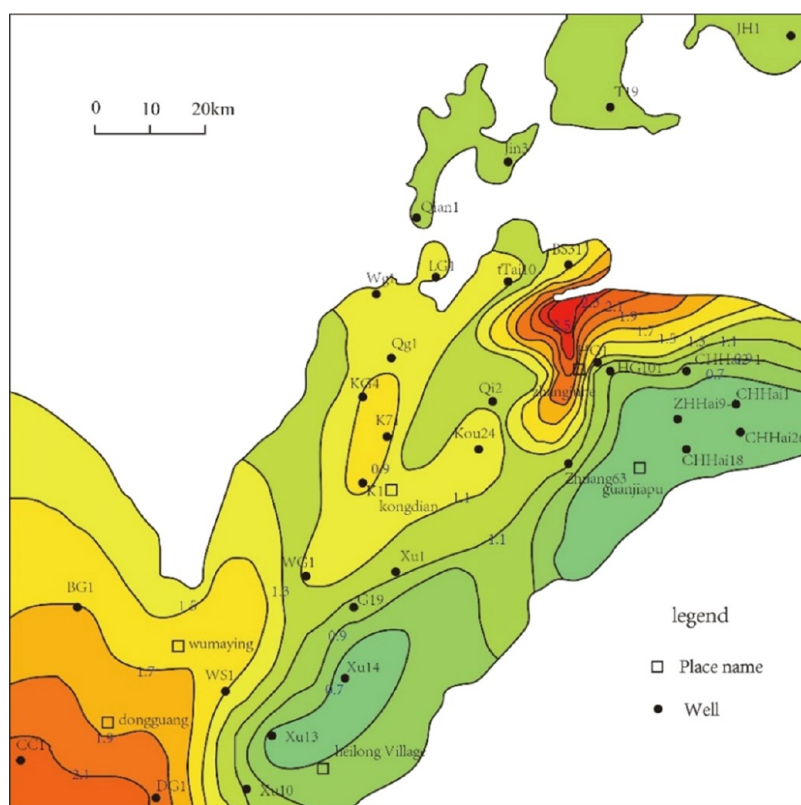


Table 3. Classification of Sedimentary Organic Facies of Carboniferous–Permian Coal Measures in Huanghua Depression^{12,42,43a}

	A	B	C	D	E	F
petrological features	terrestrial forest organic facies mainly silk charcoal and dark coal	shallow swamp forest organic facies mainly bright coal and dark coal	deep swamp forest organic facies mainly mirror coal	deep swamp reed organic facies mainly dark coal and bright coal	running water swamp organic facies mainly dark coal and spore bright coal	open water organic facies mainly composed of sapropelic coal and carbonaceous mudstone
V (%)	<25%	>50 to 85%	>85%	>50 to 70%	<50%	<50%
component characteristics	dominated by inert group	contains a large amount of stromal vitrinite	homogeneous vitrinite and structured vitrinite are more	contains a large amount of matrix vitrinite, coarse granule and sporophyte, etc.	contains a large amount of chitinic components	mainly mineral asphalt matrix and algae
biological type	mainly higher plants	mainly higher plants	mainly higher plants	mainly higher plants and their leaves	mainly higher plants and their leaves, some lower plants	mainly lower plants
sedimentary environment characteristics	mainly <1 >0.6 <2	mainly 1–10 >0.6 mainly 2–10	mainly 1 to ~50 >0.6 >10	mainly 1–10 <0.6 >5	mainly <3 <0.6 2–5	mainly 1–10 <0.6 >5
hydrodynamic conditions	above the diving surface or underwater in an oxidizing environment	still water conditions below the diving surface	underwater deposition	underwater deposition	running water underwater deposition	running water underwater deposition
swamp type	middle to high swamp	middle to high swamp	middle to low swamp	low swamp	running water swamp	low swamp
redox	oxidation	weak reduction	mainly reduction	reduction	oxidation	strong reduction
sedimentary environment	alluvial plain	coastal plain, tidal flat, delta plain	tidal flats, lagoons, delta fronts	marina shallow sea, lagoon	floodplain, tidal channel, interdelta bay	marina shallow sea, lagoon
geochemical features	<50 III mainly gas	50–100 III oil, gas	100–150 III oil, gas	>150 III–II oil, gas	>150 III–II oil, gas	100–150 I–II oil, gas
Joens' scheme	D,CD	CD/C	C,BC	C,BC,B	BC,B	B,AB,A

^aNote: Only used to describe coal seams.

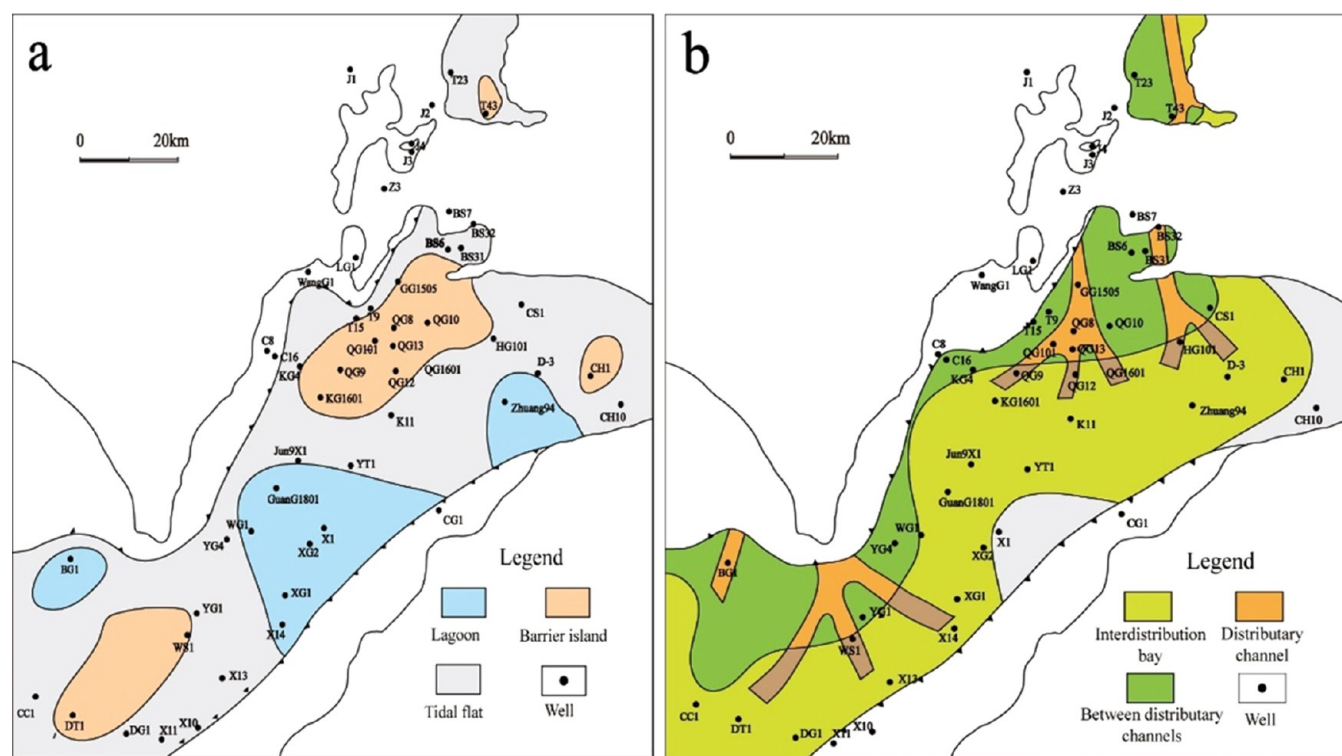


Figure 14. Sedimentary facies of (a) Taiyuan Formation and (b) Shanxi Formation in Huanghua Depression (modified after ref 45).

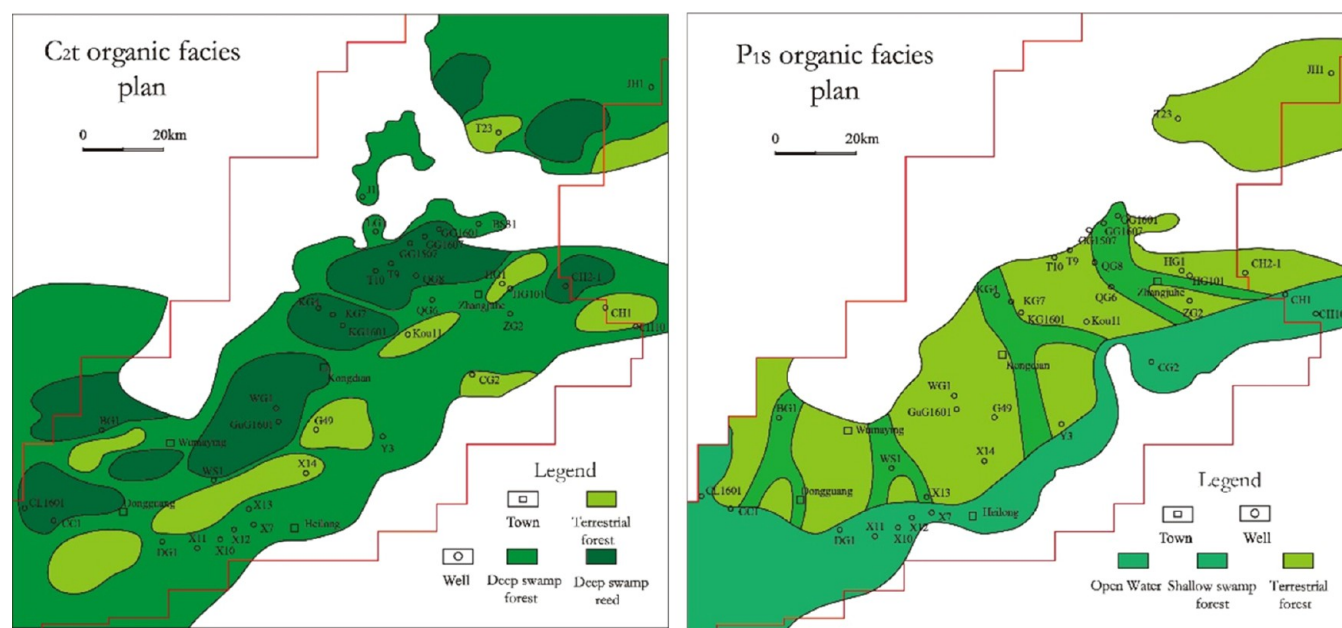


Figure 15. Planar distribution of sedimentary organic facies in Huanghua Depression.

of the depositional environment, the type and content of organic components, etc. Combined with E. Stach's (1982) understanding of the division of Carboniferous coal facies, the sedimentary organic facies of coal and mudstone in the study area are divided into: ① terrestrial forest sedimentary organic facies; ② shallow marsh forest sedimentary organic facies; ③ deep swamp forest sedimentary organic facies; ④ deep swamp reed sedimentary organic facies; ⑤ flowing water swamp sedimentary organic facies; and ⑥ open water sedimentary

organic facies. The main characteristics of the various organic facies are shown in Table 3.

4.3.2. Planar Distribution of Organic Facies. The Carboniferous–Permian coal measures in the Huanghua Depression belong to the North China Platform and are part of the coal-accumulation area in North China. Therefore, based on the changes and distribution of sedimentary organic facies, the same type of facies has the characteristics of stable distribution in a large area.^{44,45} According to the relationship between sedimentary evolution and peat swamps (Figure 14), with the

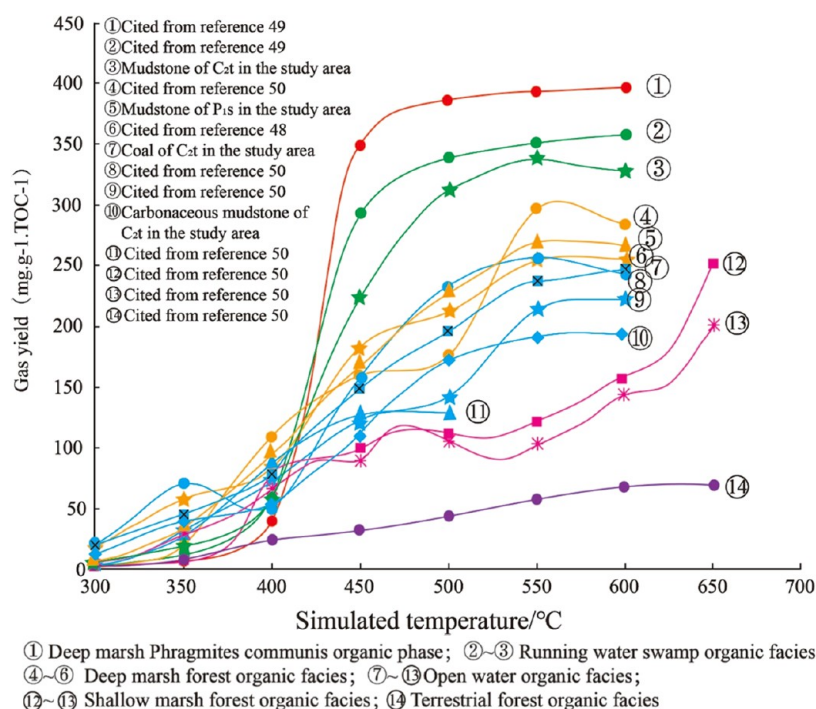


Figure 16. Hydrocarbon-generation characteristics of different organic facies.

regression of the epicontinental sea from the Late Carboniferous to the Early Permian, a large scale of peat swamps formed in the sea–land transition zones such as coastal plains, bays, and lagoons.^{42,43} The distribution laws changed with the migration of the coastline. Therefore, the distribution of different sedimentary organic facies has a certain feature of zonality. However, influenced by the change of the sedimentary base, some special sedimentary organic facies will appear in local areas. From the actual situation (Figure 15), synsedimentary uplift or tidal beach in the basin has a great influence on the variation and distribution of sedimentary organic facies and the properties of source rocks.

(1) Late carboniferous epoch

during the Benxi Period: the whole North China was divided into eastern and western sea areas under the influence of seawater intrusion along the east and west directions. At this time, the Bohai Bay Basin was still part of the whole North China block and was located in the eastern sea. From the overall distribution of the sedimentary environment, the alluvial plain, coastal plain (including beach, tidal flat, and lagoon), and carbonate platform appeared successively from north to south and had zonal distribution from north to south. The depth of the sea gradually deepened from north to south. Lagoons, barrier islands, and tidal flat facies are widely distributed in the present day. The organic facies of shallow marsh forest are widely distributed in the Huanghua area. When the Benxi Formation was deposited, there was a sedimentary organic facies of flowing water swamps in the south, while the Dongguang and Zhangjuhe areas were deep marsh reed sedimentary organic facies, and the remaining areas were mostly the shallow swamp forest organic facies. When the Taiyuan Formation was deposited, it was generally shallow marsh forest sedimentary organic facies, but there were deep marsh forest sedimentary

organic facies in Kongdian, Zhangjuhe, Wumaying, and Botou areas.

(2) The Permian

During the Shanxi period: with the reduction of the intrusion of seawater, the seawater gradually retreated from north to south. In the present-day Bohai Bay Basin, delta plain, lagoon, tidal flat, and other sedimentary environments are mainly developed. However, the Huanghua area is basically dominated by delta sediments, which are mainly manifested in further shallowing of the seawater. The shallow marsh forest sedimentary organic facies and open water sedimentary organic facies are widely developed, and only a few areas still develop some deep marsh forest sedimentary organic facies. During the deposition period of the Shihezi Formation, the seawater completely withdrew from the study area, and fluvial facies deposits were generally developed. The flowing swamp sedimentary organic facies were developed between the Xuhei and Wumaying area, and the shallow swamp forest sedimentary organic facies were still dominant in most areas. In the deposition period of the Upper Shihezi Formation, only shallow marsh forest sedimentary organic facies were developed in the study area.

4.4. Hydrocarbon-Generation Potential of Coal Measure Source Rocks. **4.4.1. Hydrocarbon-Generation Potential and Differences of Source Rocks (Coal) with Different Organic Facies.** Many scholars have carried out thermal simulation experiments of coal for hydrocarbon generation. Although there are differences in the conditions of hydrocarbon-generation simulation experiments, the final hydrocarbon production rate still depends on the material composition of coal and the type of sedimentary organic facies.^{12,28,46} Figure 16 shows the results of thermal simulation experiments for hydrocarbon generation of source rocks with different macerals. It can be seen that there are significant

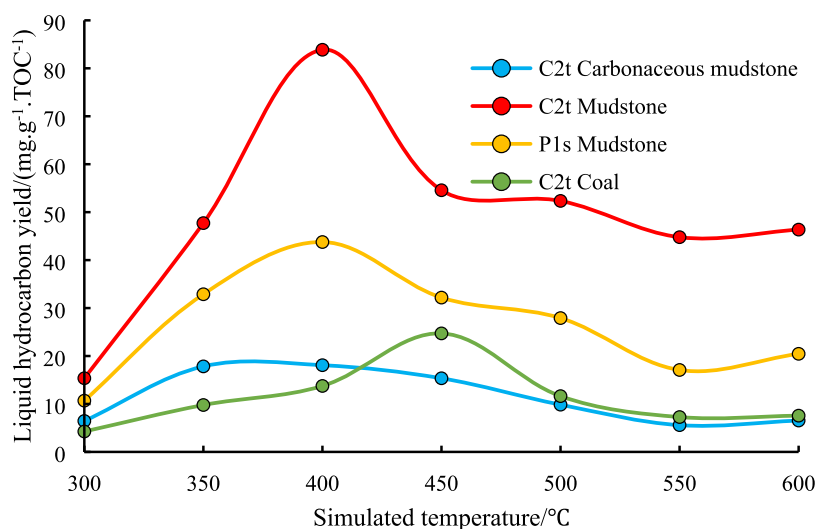


Figure 17. Comparison of the oil-generating potential of Upper Paleozoic source rocks in the study area under the thermal simulation experiment.

differences in the hydrocarbon-generation potential of different organic facies.

- (1) The gas production rate of bark coal in the organic facies of deep marsh reed can reach up to 400 mg/(g·TOC), and the gas production rate of algal candle coal in flowing water marsh is 350–400 mg/(g·TOC). The final hydrocarbon production rate of Taiyuan Formation and Shanxi Formation coal in the Ordos Basin is 100–200 mg/(g·TOC), which belongs to the organic facies of deep swamp forests. The gaseous hydrocarbon yield of terrestrial forest organic coal is only about 50 mg/(g·TOC). The hydrocarbon yield of Taiyuan Formation mudstone in the flowing water swamp organic facies in the study area is 340 mg/(g·TOC). The hydrocarbon yield in the Shanxi Formation mudstone in the deep swamp forest organic facies can reach 265 mg/(g·TOC), and that of Taiyuan Formation coal and Taiyuan Formation carbonaceous mudstone in the organic facies of shallow marsh forest is about 200 mg/(g·TOC). It can be seen that the order of hydrocarbon-generation potential from high to low is deep marsh reed, flowing swamp, deep marsh forest, open water, shallow marsh forest, and terrestrial forest. The coal samples of the Taiyuan Formation used in this experiment belong to the organic facies of shallow swamp forest. The gas production rate in the experiment is greater than that of the organic facies coal of shallow swamp forest in the Shanxi Formation and Taiyuan Formation in the Ordos Basin. It is between the coal of the organic facies in the open water and the sapropelite candle coal mainly composed of sporophytes and sapropelite in Ordos Basin, and equivalent to the hydrocarbon-generation capacity of type III–II organic matter.
- (2) With the increase of temperature, the hydrocarbon-generation process of coal samples with different organic facies also has obvious differences. From the evolution characteristics of thermal simulation product yields, the evolution process of hydrocarbon generation of deep marsh forest organic facies, open water organic facies, and shallow marsh forest organic facies has obvious multistage characteristics, which is mainly caused by the complexity of organic maceral of coal samples in each

organic facies. The organic matter of each organic facies contains not only hydrogen-rich components such as exinite and hydrogen-rich vitrinite but also relatively hydrogen-poor components such as telocollinite and inertinite. Due to the differences in the chemical structure and thermal evolution characteristics of different maceral, the hydrocarbon-generation evolution process of vitrinite humic coal samples presents several distinct evolution stages. Correspondingly, the organic facies of deep marsh reed, flowing water swamp, and terrestrial forest are relatively simple in maceral, so the stages are inconspicuous.

- (3) During the thermal simulation experiment, the width of the main hydrocarbon zone of different organic coal samples is also different. It can be seen from Figure 16 that the hydrocarbon-generation zone of the terrestrial forest coal sample is the widest. Within the range of 300–600 °C, the yield of thermal simulation products gradually increases with the increase of temperature, indicating that hydrocarbon generation occurs in all coal samples in this range, but the overall hydrocarbon generation is low. The hydrocarbon-generation zone of coal samples in the shallow marsh forest is very narrow. The hydrocarbon generation mainly occurs in the range of 400–500 °C, and the hydrocarbon generation in the other temperature ranges is quite weak. The width of the hydrocarbon-generation zone of other organic facies coal samples is between the above two and have multiple stages. The difference in the width of the hydrocarbon-generation zone is caused by the difference in the chemical structure of each coal sample. The kerogen chemical structure of source rocks in deep marsh forest organic facies, open water organic facies, and shallow marsh forest organic facies is relatively complex, including aromatic structures, bridge bonds, aliphatic substituents of different lengths, and various types of heteroatom functional groups, and the distribution range of bond energy is large, so the temperature range of hydrocarbon generation enhanced by thermal action is also large, and the corresponding chemical bonds react at each temperature, resulting in a wide hydrocarbon-generation zone. On the contrary, the main hydro-

carbon-generation maceral of the organic facies in the deep marsh reed is the exinite group, and its chemical structure is more homogeneous, so the hydrocarbon-generation reaction is more concentrated. In addition, the content of the aromatic structure of organic matter in the organic facies of deep marsh reed is low, so its chemical bond energy is generally low. The hydrocarbon generation substantially ends at 450 °C, and the hydrocarbon generation is quite weak at a high temperature. Different from the shallow marsh forest organic facies, coal samples still have considerable hydrocarbon-generation potential in the over-mature stage (>500 °C).

4.4.2. Discussion on Hydrocarbon-Generation Potential of Coal Measure Source Rocks. Thermal simulation results show that the Upper Paleozoic coal in Huanghua Depression has not only coal-formed gas generation potential but also coal-to-oil-generation potential (Figure 16). The Middle–Lower Jurassic coal measures in the Tu Ha Basin are considered to be typical coal-to-oil basins in which the volume fraction of vitrinite is generally 60–80%, and the volume fractions of inertinite and exinite are 10–25 and 5–15%, respectively. Hydrogen-rich organic macerals are mainly xyloplasts, keratinites, and resinites, and hydrogen-rich stromal vitrinites.^{47–49} The composition characteristics of this maceral are very similar to those of Upper Paleozoic coal in Huanghua Depression. On the whole, organic facies is also dominated by open water organic facies and shallow marsh forest organic facies. The thermal simulation experiment results (Figure 17) show that the Ro value of coal samples in Taiyuan Formation in the study area is 0.62%, and the maximum oil-generation rate is 24.71 mg/(g·TOC). The Ro value of carbonaceous mudstone samples in Taiyuan Formation in the study area is 0.63%, and the maximum oil-generation rate is 18.08mg/(g·TOC). The maximum oil-generation rates of dark mudstones in the Taiyuan Formation and Shanxi Formation in the study area are 83.67 mg/(g·TOC) and 43.77 mg/(g·TOC), respectively. Therefore, the Taiyuan Formation and Shanxi Formation coal-bearing source rocks in the study area have certain oil-generating potential, and the oil-generating potential of dark mudstone is greater than that of carbonaceous mudstone and coal.

The Upper Paleozoic coal seam in Huanghua Depression is thick, widely distributed, and high in organic matter content. From the perspective of the total amount of organic matter, the hydrocarbon-generation potential of the Upper Paleozoic coal in the Huanghua Depression cannot be ignored. Coal may be one of the important source rocks in the Huanghua Depression. At the same time, the dark mudstone is also well developed, and its hydrocarbon-generation potential is equivalent to that of type I and type II kerogen. Moreover, although the coal-bearing strata of the Taiyuan Formation and Shanxi Formation mainly develop open water organic facies and shallow marsh forest organic facies; some thin coal seams or micro coal layers develop hydrogen-rich organic facies, which have the potential of type II kerogen to generate oil and gas. Therefore, the coal-bearing source rocks of Upper Paleozoic in the Huanghua Depression are good and have an extremely high hydrocarbon-generation potential.

Due to the differences in the thermal evolution degree of the Upper Paleozoic in Huanghua Depression, there may be great discrepancies in oil and gas generation in each area. It can be

roughly judged from the distribution characteristics of current vitrinite reflectance. Heilongcun area has low maturity and hydrocarbon production rate. The Ro value of source rock in the Kongdian and Wumaying area is about 1.0%, which is in the peak period of liquid hydrocarbon generation, and the yield of coal-to-oil is relatively high. Zhangjuhe and Dongguang areas are highly over-mature and have high coal-to-gas potential, but due to the influence of magmatism, their coal-to-gas potential needs to be evaluated.

5. CONCLUSIONS

- (1) The Upper Paleozoic source rocks in the Huanghua Depression have good hydrocarbon-generation capacity. The abundance of organic matter in source rocks of the Taiyuan Formation is higher than that of the Shanxi Formation. Compared with coal and mudstone of the Shanxi Formation, the content of hydrocarbon-generating components in coal and mudstone of the Taiyuan Formation is higher.
- (2) The sedimentary organic facies in the study area can be divided into the following: ① terrestrial forest sedimentary organic facies; ② shallow swamp forest sedimentary organic facies; ③ deep swamp forest sedimentary organic facies; ④ deep swamp reed sedimentary organic facies; ⑤ flowing water swamp sedimentary organic facies; and ⑥ open water sedimentary organic facies. The Taiyuan Formation mainly develops organic facies of flowing water swamp, deep swamp forest, and shallow swamp forest, with strong hydrocarbon-generation capacity, while the Shanxi Formation mainly develops organic facies of deep swamp forest and shallow swamp forest.
- (3) The complexity of the organic maceral of coal sample in each organic facies results in obvious differences in the hydrocarbon-generation process and hydrocarbon-generation potential. The order of hydrocarbon-generation potential from high to low is deep marsh reed organic facies, flowing swamp organic facies, deep marsh forest organic facies, open water organic facies, shallow marsh forest organic facies, and terrestrial forest organic facies.
- (4) The results show that the coal-bearing source rocks of the Taiyuan Formation and Shanxi Formation in the study area have a certain oil-generation potential, and the oil-generation potential of mudstone is greater than that of carbonaceous mudstone and coal. The Ro of source rocks in the study area of Kongdian and Wumaying is about 1.0%, which is in the peak period of liquid hydrocarbon generation, and the coal-to-oil yield is relatively high.

AUTHOR INFORMATION

Corresponding Author

Jianhui Zeng — State Key Laboratory of Petroleum Resources and Prospecting, China University of Petroleum (Beijing), Beijing 102249, China; College of Geosciences, China University of Petroleum (Beijing), Beijing 102249, China; orcid.org/0000-0003-4768-043X; Email: zengjh1215@163.com

Authors

Chuanming Li — State Key Laboratory of Petroleum Resources and Prospecting, China University of Petroleum (Beijing),

Beijing 102249, China; College of Geosciences, China University of Petroleum (Beijing), Beijing 102249, China; orcid.org/0000-0001-9877-5581

Haitao Liu – Research Institute of Petroleum Exploration and Development, Beijing 100083, China

Hongjun Li – Research Institute of Petroleum Exploration and Development, Dagang Oilfield Company, CNPC, Tianjin 300280, China

Xiaoqing Bu – State Key Laboratory of Petroleum Resources and Prospecting, China University of Petroleum (Beijing), Beijing 102249, China; College of Geosciences, China University of Petroleum (Beijing), Beijing 102249, China

Shuning Liu – State Key Laboratory of Petroleum Resources and Prospecting, China University of Petroleum (Beijing), Beijing 102249, China; College of Geosciences, China University of Petroleum (Beijing), Beijing 102249, China

Complete contact information is available at:

<https://pubs.acs.org/10.1021/acsomega.3c03400>

Notes

The authors declare no competing financial interest.

This article references 53 other publications.

ACKNOWLEDGMENTS

C.L. was employed by the College of Geoscience, China University of Petroleum, Beijing, China. The remaining authors declare that the research was conducted in the absence of any commercial or financial relationships that could be construed as a potential conflict of interest. This work is financially supported by the grants from the National Natural Science Foundation of China (No. 41972147).

REFERENCES

- (1) Rogers, M. A. Application of Organic Facies Concepts to Hydrocarbon Source Rock Evaluation, Proceedings of the 10th World Petroleum Congress. Romania; OnePetro, 1979; pp 23–29.
- (2) Diessel, C. F. K. The stratigraphic distribution of inertinite. *Int. J. Coal Geol.* **2010**, *81*, 251–268.
- (3) Ge, Z. R. *Evaluation of Carboniferous Permian Source Rocks in Huanghua Depression*; Northeast Petrol. University: Heilongjiang, 2017.
- (4) Altunsoy, M.; Ozdogan, M.; Ozcelik, O.; Unal, N. Organic facies characteristics of the Pliocene coaly units, Central Anatolia, Ilgin (Konya/Turkey). *Energy Procedia* **2015**, *76*, 33–39.
- (5) Alipour, M. Organic facies and paleo-depositional environments of the Aptian-Albian Kazhdumi source rock in the Zagros basin of Iran. *Mar. Pet. Geol.* **2022**, *145*, No. 105887.
- (6) Jones, R. W. Organic Facies. *Adv. pet. Geoch.* 1987, 2.
- (7) Bishop, A. N.; Abbott, G. D. Vitrinite reflectance and molecular geochemistry of Jurassic sediments: the influence of heating by Tertiary dykes (northwest Scotland). *Org. Geochem.* **1995**, *22*, 165–177.
- (8) Ruppel, S. C.; Rowe, H.; Milliken, K.; Gao, C.; Wan, Y. P. Facies, rock attributes, stratigraphy, and depositional environments: Yanchang Formation, Central Ordos Basin, China. *Interpretation* **2017**, *5*, SF15–SF29.
- (9) Alizadeh, B.; Najjari, S.; Kadkhodaie-Ilkhchi, A. Artificial neural network modeling and cluster analysis for organic facies and burial history estimation using well log data: A case study of the South Pars Gas Field, Persian Gulf, Iran. *Comput. Geosci.* **2012**, *45*, 261–269.
- (10) Ehsan, M.; Gu, H.; Ali, A.; Akhtar, M. M.; Abbasi, S. S.; et al. An integrated approach to evaluate the unconventional hydrocarbon generation potential of the Lower Goru Formation (Cretaceous) in Southern Lower Indus basin, Pakistan. *J. Earth Syst. Sci.* **2021**, *130*, No. 90.

(11) Ni, Y. Y.; Liao, F. R.; Gao, J. L.; Chen, J. P.; Yao, L. M.; Zhang, D. J. Hydrogen isotopes of hydrocarbon gases from different organic facies of the Zhongba gas field, Sichuan Basin, China. *J. Pet. Sci. Eng.* **2019**, *179*, 776–786.

(12) Shao, L. Y.; Dong, D. X.; Li, M. P.; Wang, H. S.; Wang, D. D.; Lu, J.; Zheng, M. Q.; Cheng, A. G. Sequence-paleogeography and coal accumulation of the Carboniferous–Permian in the North China Basin. *J. China Coal Soc* **2014**, *39*, 1725–1734.

(13) Diessel, C. *On the Correlation between Coal Facies and Depositional Environments*; University of Newcastle: Australia, 1986; pp 19–22.

(14) Diessel, C. F. K. Utility of coal petrology for sequence stratigraphic analysis. *Int. J. Coal Geol.* **2007**, *70*, 3–34.

(15) Wang, J. L.; Zheng, H. R. Potential of remaining hydrocarbon resources and main exploration domains in eastern mature exploration areas in Eastern China. *Oil Gas Geol.* **2003**, *24*, 296–300.

(16) Jin, K. L.; Liu, D. M.; Xiao, X. M.; Li, S. Z.; Tu, J. Q.; Yao, S. P. The organic composition, ultrastructural and geochemical characteristics of China's oil and gas source rocks and their hydrocarbon generation rules. *Coal Geol. China* **1995**, *7*, 47–51.

(17) Jones, R. W. *Organic Facies. Welte D. Advances in Petroleum Geochemistry II Brooks J*; Academic press: London, 1987; pp 1–90.

(18) Li, S. G.; Wu, T. *China Petroleum Geology Record (Vol.4): Dagang Oilfield*; Petroleum Industry Press: Beijing, 1987; pp 1–417.

(19) Wu, Y. P.; Yu, X. M. Natural gas resource potential and the strategy of exploration and development in Huanghua Depression. *Nat. Gas Geosci.* **2003**, *14*, 235–239.

(20) Haven, H. L. t.; de Leeuw, J. W.; Rullkötter, J. Restricted utility of the pristane/phytane ratio as a palaeoenvironmental indicator. *Nature* **1987**, *330*, 641–643.

(21) Fu, L. X. *Petroleum System Related to Paleozoic Group in Dagang Exploratory Area*; Petrochina Research Institute of Pet. Exp. Dev.: Beijing, 2001; pp 51–86.

(22) Hu, T.; Pang, X.; Jiang, F.; Zhang, C.; Wu, G.; Hu, M.; Jiang, L.; et al. Dynamic continuous hydrocarbon accumulation (DCHA): Existing theories and a new unified accumulation model. *Earth-Sci. Rev.* **2022**, *232*, No. 104109.

(23) Xiao, S. B.; Gao, X. L.; Jiang, Z. X.; Qiao, H. S. Cenozoic dextral strike-slip motion in Bohai bay basin and its meaning to petroleum geology. *Geotecton. Metallog.* **2000**, *24*, 321–328.

(24) Chi, Y. L.; Zhao, W. Z. Strike-slip deformation during the cenozoic and its influence on hydrocarbon accumulation in the Bohai bay basin. *Acta Pet. Sin.* **2000**, *21*, 14–20.

(25) Yang, R. Z.; Liu, H. T.; Li, H. J.; Zhao, C. Y.; Li, C. M. Accumulation mechanism and model of coal measure derived oil and gas in the deepreservoir of Huanghua Depression, Bohai Bay Basin. *Nat. Gas Geosci.* **2022**, *33*, 1074–1090.

(26) Zhao, X. Z.; Li, H. J.; Fu, L. X.; Cui, Y.; Han, G. M.; Lou, D.; Pu, X. G.; Liu, G. Q.; Jiang, W. Y.; Dong, X. Y.; Zou, L. L. Characteristics, main controlling factors and development mode of Paleozoic coal-formed condensate gas reservoirs in Huanghua depression, Bohai Bay Basin. *Acta Pet. Sin.* **2021**, *42*, 1592–1604.

(27) Gao, X. X. *Geology of Petroleum and Gas in the Huanghua Depression. Beijing: Pet. Ind. Press* **1997**, 1–7.

(28) Hou, Z. S.; Chen, S. Y.; Yan, J. H. Sedimentary Characteristics and Controlling Factors of Upper Paleozoic in Dagang Exploration Area. *Earth Sci.* **2017**, *42*, 2055–2068.

(29) Wang, Z. Y.; He, H. Q.; Cheng, K. M. Exploration prospect of Paleozoic primary oil and gas pools in Huabei area. *Acta Pet. Sin.* **1999**, *20*, 1–6.

(30) Hu, T.; Pang, X. Q.; Xu, T. W.; Li, C. R.; et al. Identifying the key source rocks in heterogeneous saline lacustrine shales: Paleogene shales in the Dongpu depression, Bohai Bay Basin, eastern China. *AAPG Bull.* **2022**, *106*, 1325–1356.

(31) Fu, L. X.; Lou, D.; Li, H. J. The Control of Indosinian Yanshan Movement on the Formation of Buried Hills in Dagang Exploration Area. *Acta Pet. Sin.* **2016**, *37*, 19–30.

- (32) Zhang, F. P.; Wu, Z. P.; Li, W. Structural Characteristics and Evolution of Indosinian Yanshanian in Huanghua Depression. *J. China Univ. Min. Technol.* **2019**, *48*, 842–857.
- (33) SY/T5124-1995, Determination of vitrinite reflectance in sedimentary rock [S].
- (34) ICCP. The new inertinite classification (ICCP System, 1994). *Fuel* **2001**, *80*, 459–471.
- (35) GB/T 18062-2012, Rock pyrolysis analysis [S].
- (36) Chen, J. P.; Zhao, C. Y.; He, Z. H. Discussion on evaluation criteria for hydrocarbon generation potential of organic matter in coal measures. *Pet. Exp. Dev.* **1997**, *24*, 1–5.
- (37) Zhang, H. F.; Fang, C. L.; Zhang, Z. H. *Petroleum Geology*; Pet. Ind. Press, 1999.
- (38) Chen, R. S. *Petroleum and Natural Gas Geology*; China University of Geosci. Press, 1994.
- (39) Gu, L.; Dai, T. G.; Fan, W. M. Petrographic and petrochemical characteristics of the Mesozoic-Cenozoic volcanic rocks in Huanghua basin. *Acta Geol. Sin.* **2000**, *21*, 365–372.
- (40) Qu, X. R.; Zhu, Y. M.; Li, W.; Tang, X.; Zhang, H. Evaluation of hydrocarbons generated from the Permo-Carboniferous source rocks in Huanghua Depression of the Bohai Bay Basin, China. *Energy Explor. Exploit.* **2018**, *36*, 1229–1244.
- (41) Fan, J. L.; Huang, Z. Q.; Fan, W. H. Cenozoic tectonic evolution of qikou sag and its relations to hydrocarbon traps in Bohai bay basin of east China. *J. Jilin Univ., Earth Sci. Ed.* **2004**, *34*, 536–541.
- (42) Shao, L. Y.; He, Z. P.; Lu, J. *Sequence Stratigraphy and Coal Accumulation of the Carboniferous and Permian in the Western Peri-Bohai Bay Area of the Northern China*; Geological Publishing House: Beijing, 2008; p 174.
- (43) Shao, L. Y.; Wang, X. T.; Wang, D. D.; Li, M. P.; Wang, S.; Li, Y. J.; Shao, K.; Zhang, C.; Gao, C. X.; Dong, D. X.; Cheng, A. G.; Lu, J.; Ji, C. W.; Gao, D. Sequence stratigraphy, paleogeography, and coal accumulation regularity of major coal-accumulating periods in China. *Int. J. Coal Sci. Technol.* **2020**, *7*, 240–262.
- (44) Sang, S. X. Analysis of coalbed methane exploration prospect in junggar basin. *Nat. Gas Ind.* **2005**, *25*, 13–15.
- (45) Liu, D. G.; Wu, X. Z.; Zhao, Z. Y. Coal bed methane resource potential and exploration area selection in Junggar basin. *Xinjiang Pet. Geol.* **2007**, *6*, 273–275.
- (46) Wang, F. C. *Sedimentary Facies Analysis and Reservoir Research of Upper Paleozoic in the Middle South of Dagang Oilfield*, Jingzhou. Changjiang University, 2014.
- (47) Shi, J. The study on the law of light coal, algal candle coal and bark coal in South China's Longtan coal system. *Coal Geol. China* **1993**, *5*, 23–27.
- (48) Xiang, L. *Simulation Experiment Study on the Difference of Humic Coal Gas Generating Potential of Different Environmental Origin*; Changjiang University: Jingzhou, 2015.
- (49) Feng, Y.; Huang, Z. L.; Wang, F. Z.; Zhang, H.; Li, T. J.; Liang, Y. The hydrocarbon generation and expulsion features of source rocks and tight oil potential of the second member of the Qiketai Formation, Shengbei area in the Turpan-Hami Basin, NW China. *Geol. J.* **2021**, *56*, 337–358.